Visualization of the vortex-mediated pinning of ferromagnetic domains in superconductor-ferromagnet hybrids

J. Fritzsche,* R. B. G. Kramer, and V. V. Moshchalkov
INPAC-Institute for Nanoscale Physics and Chemistry, Katholieke Universiteit Leuven, Celestijnenlaan 200 D, B-3001 Leuven, Belgium
(Received 22 December 2008; revised manuscript received 23 February 2009; published 1 April 2009)

A thin superconducting (S) film reduces the mobility of magnetic domains in an underlying ferromagnet (F). The magnetic domain pattern of a barium hexaferrite single crystal was imaged as a function of temperature and external magnetic field, in both presence and absence of a covering niobium film. Comparative analysis of these two cases reveals that the relaxation of the domains is hampered, if the external field is changed while the Nb-film is superconducting. This effect in the S/F hybrids is interpreted in terms of a vortex-mediated pinning of magnetic domains by pinning centers in the superconductor.

DOI: 10.1103/PhysRevB.79.132501 PACS number(s): 74.78.Db, 75.60.−d, 74.25.Qt

Based on the opposed nature of superconductivity and ferromagnetism, a wealth of physical phenomena arises from the interaction of these two states when existing side by side. One option to achieve such coexistence is the preparation of superconductor/ferromagnet (S/F) hybrid systems,[1–3] where the two components form an artificial entity that allows for their mutual interaction. In the particular case of hybrids with spatially separated S and F components, the exchange of electrons and Cooper pairs is suppressed, limiting the interaction to magnetic coupling via stray magnetic fields. A great deal of work has been carried out on such S/F hybrids with purely magnetic coupling, mainly focusing on the *unilateral* manipulation of the superconducting state with the help of the ferromagnet. For instance, the remarkable phenomena of domain-wall superconductivity[4] or vortex pinning by magnetic objects[5,6] are related to an influence from the ferromagnet on the superconductor. However, not only from a fundamental point of view, but also in regard to potential applications in which superconductivity is controlled by ferromagnets, it is of great interest to study *the reverse*, i.e., the *influence of the superconductor on the ferromagnet*.

Nevertheless, to this day, there are not more than a few tens of publications on the *mutual* electromagnetic interaction between the two subsystems in S/F hybrids. Among these studies, most are of theoretical nature, predicting surprising effects such as shrinking of magnetic domain walls[7] and of the magnetic domain structures,[5,8,9] or the spontaneous formation of vortices and magnetic domains.[10] Experimentally, it has been demonstrated that screening currents can spontaneously change the distribution of the magnetization in submicron systems,[11] and that sandwiching superconductors can alter the magnetic state of ferromagnets in multilayer structures.[12]

In this work we present a direct visualization of the influence of the superconductor on the ferromagnet in an S/F hybrid system. To do so, it is necessary to observe the behavior of the magnetic domains in the ferromagnet for two cases: once in presence and once in absence of superconductivity. Accordingly, the approach of this study was to image the magnetic domain pattern of the ferromagnet as a function of the state of the superconductor. In particular, for various external fields and temperatures, scanning Hall-Probe microscopy (SHPM) (Ref. 13) was performed on the basal plane of a barium hexaferrite single crystal ($BaFe_{12}O_{19}$), which was partly covered by 100 nm of niobium. The ferromagnetic crystal was grown from a sodium carbonate flux,[14] and subsequently mechanically polished until a peak-to-peak roughness below 2 nm was achieved. Thereafter, an electrically insulating layer of 10 nm silicon dioxide was magnetron sputtered on the polished surface, followed by the electron-beam evaporation of 100 nm of niobium. The superconductor was then partly removed via electron-beam lithography and dry etching, such that a millimeter sized square together with a transport bridge remained on top of the ferromagnet. This particular design of the sample allowed for imaging of the magnetic domain pattern with and without the covering niobium film at two locations $\mathcal{P}$ and $\mathcal{Q}$, respectively (see the illustration of Fig. 1). In addition, the used SHPM made it possible to move *in situ* between the two locations. Moreover, the transport bridge allowed to detect the phase boundary between the superconducting and normal state of the S-layer as shown in Fig. 1 ($T_{c0} \simeq 7.5$ K).

SHPM imaging of the sample at low temperatures (see Fig. 2) revealed sections of the well-known domain pattern of single crystals of $BaFe_{12}O_{19}$ (Ref. 15) (see also the inset of Fig. 1), resulting from domain branching toward the

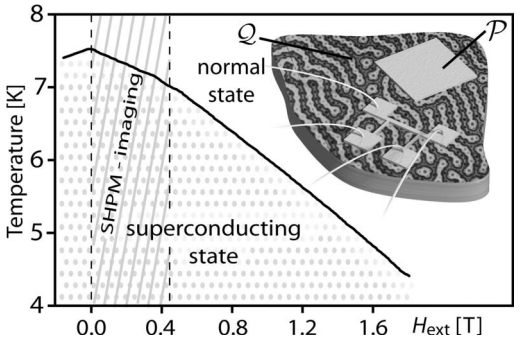

FIG. 1. The phase boundary between normal and superconducting state of the transport bridge, defined by 50% of the resistance in the normal state. A hatched area indicates the region where SHPM imaging was performed. The inset illustrates the processed sample with the two locations $\mathcal{P}$ and $\mathcal{Q}$, and a transport bridge on top of the ferromagnet. (Note that the image of the magnetic domain pattern, obtained by polarized light microscopy, is not in scale with the sketched structure.)

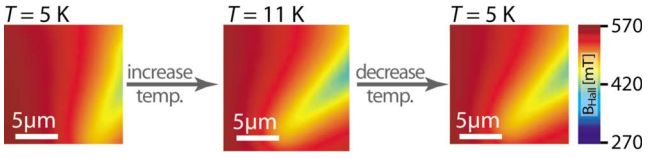

FIG. 2. (Color online) SHPM images of the magnetic domains in the $BaFe_{12}O_{19}$ substrate at $\mu_0 H_{ext}$=420 mT, obtained successively at 5 K (left), 11 K (middle), and again 5 K (right).

surface.[16] However, no signs of vortices were observed, suggesting that only the magnetic signal of the ferromagnet is seen in the SHPM images. This conclusion is reasonable due to the high vortex density (100 mT corresponds to 50 vortices/μm^2), the size of the Hall probe (600 $\times$600 nm^2) and the distance of $\sim$800 nm between Hall probe and sample surface during the scan. Surprisingly, changes in the magnetic domain structure were sometimes observed, caused by an increase in temperature by a few degrees while keeping the external magnetic field *constant* (see the first two SHPM images of Fig. 2). This effect proved to be irreversible, in that the original domain configuration could not be recovered by reducing the temperature again (see the last two SHPM images of Fig. 2). Moreover, it became apparent that this instability of magnetic domains to rise in temperature could systematically be induced, but not unless the temperature was lowered to the base temperature of the cryostat (4.2 K) prior to changing the external field.

To get to the origin of these observations and to reveal the role of the superconductor in this process, systematic series of domain images were recorded at both locations $\mathcal{P}$ and $\mathcal{Q}$. Thereby, the external magnetic field H_{ext} was reduced in steps of 5 mT from almost saturation (475 mT) to remanence (0 mT). Between succeeding values of H_{ext}, two sequences of SHPM images were taken (see Fig. 3), each of them imaging the $BaFe_{12}O_{19}$ domain structure at 5, 7, 9, and 11 K. Finally, before switching over to the following external field value, the sample was cooled down to 4.2 K, ensuring that H_{ext} changed only at the lowest temperature.

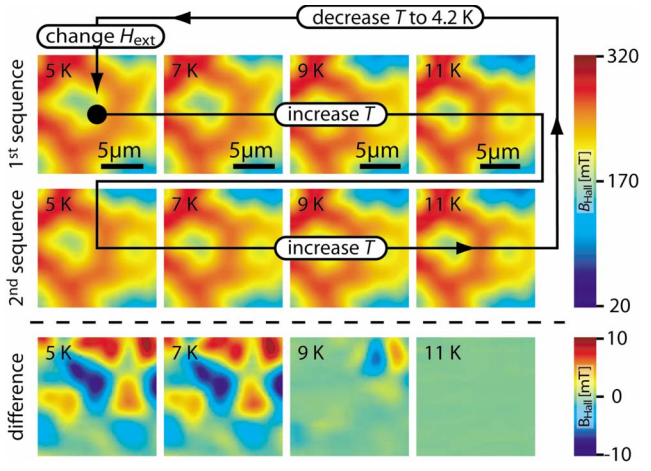

FIG. 3. (Color online) Illustration of a systematic series of SHPM images. Top and middle row: images of the magnetic domains in the substrate during the first and second temperature sequence, respectively ($\mu_0 H_{ext}$=170 mT). Bottom row: differences between the domain images of the first and second sequence.

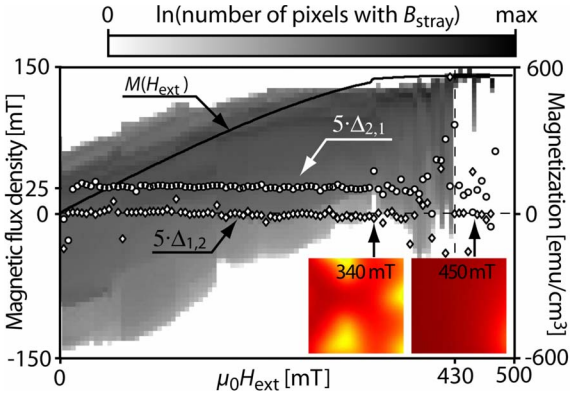

FIG. 4. (Color online) The distribution of B_{stray} found in the SHPM images, obtained at 5 K during the first imaging sequences. The solid line shows the bulk magnetization $M(H_{ext})$ of the substrate at 5 K. Markers indicate the differences $\Delta_{1,2}$ and $\Delta_{2,1}$ between the averages of the 5K images obtained during the first and second sequence at the same H_{ext} (diamonds) and during the second and first sequence at subsequent fields (circles).

It is instructive to first check the consistence of the SHPM images with global magnetic properties of the substrate. To do so, all images obtained at 5 K during the first sequences at location $\mathcal{P}$ were analyzed and correlated with the bulk magnetization $M(H_{ext})$ of the $BaFe_{12}O_{19}$ crystal, obtained from vibrating sample magnetometry for an decreasing external field (Fig. 3). Here, the distribution of the z component B_{stray} of the stray field of the substrate, found in the Hall-probe images, is shown. (Note, that $B_{stray}=B_{Hall}-\mu_0 H_{ext}$ with the measured flux density B_{Hall}.) In this diagram, as indicated by the example of the images taken at 340 and 450 mT, each column shows the analysis of one specific SHPM image. From Fig. 4 it becomes clear that the distribution of B_{stray} follows—to a certain degree—the magnetization M of the crystal. This observation reflects directly that the observed domains do not extend deep into the crystals' bulk,[16] but are confined to a shallow region at the surface. Hence, for ever higher values of M, the stray fields of parallel and reverse domains are increasingly enhanced and compensated, respectively, by the field of the underlying domains in the bulk material. The SHPM image of 340 mT illustrates these circumstances particularly well, since values of B_{stray} are positive without exception, yet several reverse domains are clearly visible. Furthermore, in accordance with a small but finite slope of $M(H_{ext})$, reverse domains exist for high external fields (e.g., $\mu_0 H_{ext}>400$ mT), as can be seen from the image taken at 450 mT. The chance, however, that one of them falls within the scanned area, is seemingly small. Summing up, the global magnetization of the substrate is reflected in the SHPM images despite the presence of the superconductor.

Now, in order to reveal from the SHPM images the role of the superconductor in the above described effect, it is necessary to compare the domain images for $T<T_c$ with those for $T>T_c$ for both cases, with and without the Nb film. Unfortunately, images at different temperatures can hardly be compared due to the view size changing with temperature. However, as mentioned above, the fluctuations of magnetic

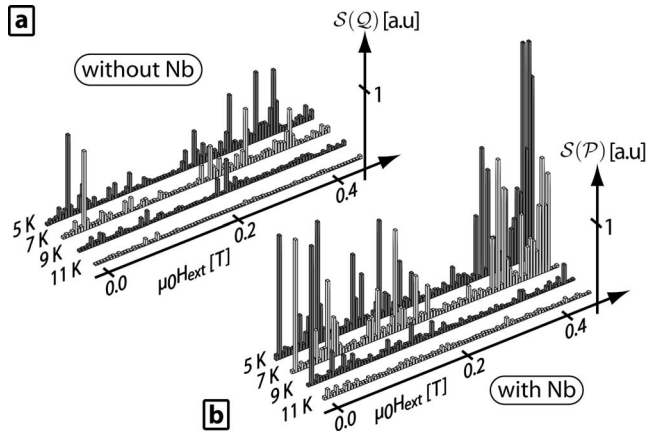

FIG. 5. Statistics of the instability of magnetic domains to temperature rise. For all investigated values of T and H_{ext}, the measure $\mathcal{S}$ [Eq. (1)] is shown for (a), location $\mathcal{Q}$ (without S layer) and (b), location $\mathcal{P}$ (with S layer).

domains proved to be irreversible to changes in temperature. Therefore, the difference between corresponding images (i.e., at the same T) of the first and the second temperature sequence shows precisely for which amount the domain pattern changed during the first sequence (see the bottom row of Fig. 3). Accordingly, the sum $\mathcal{S}$ of the absolute values of these differential images,

$$\mathcal{S}_n := \sum_{i,j=1}^{128} |\mathrm{pix}_{i,j}(T_n, 1^{\mathrm{st}}\mathrm{seq.}) - \mathrm{pix}_{i,j}(T_n, 2^{\mathrm{nd}}\mathrm{seq.})|, \qquad (1)$$

with $T_n \in \{5\ \mathrm{K}, 7\ \mathrm{K}, 9\ \mathrm{K}, 11\ \mathrm{K}\}$, was defined as a measure of how much the magnetic domain pattern changed between the first and the second sequence.

The values of the measure $\mathcal{S}(H_{ext}, T)$ were extracted from the two series of measurements performed at location $\mathcal{P}$ and $\mathcal{Q}$. From the corresponding diagrams (Fig. 5), a substantial difference between the two cases emerges already at first glance, since more and generally higher peaks are seen when the superconductor is present. Moreover, by far the biggest differences between $\mathcal{S}(\mathcal{P})$ and $\mathcal{S}(\mathcal{Q})$ occur at the two lowest temperatures of 5 and 7 K, when the niobium layer at $\mathcal{P}$ is superconducting (see Fig. 1). Nevertheless, for a certain number of measurements on the bare crystal, $\mathcal{S}$ shows higher values too, indicating that at this location, similar but less frequent changes in the magnetic configuration occur during the first sequence of imaging.

From the above observations it is clear that when changing the external field at the base temperature, there was a certain probability for the magnetic domains in the substrate not to reach their new equilibrium, unless the temperature increased sufficiently. This is valid for both cases, with and without the covering niobium film. It is reasonable to attribute that effect to a certain pinning of the magnetic domains by structural defects[17] in the $BaFe_{12}O_{19}$ crystal. This pinning, effective at the base temperature, could then be overcome by thermal activation when the temperature increased, resulting in high values of $\mathcal{S}$ in Fig. 5(a). However, the niobium film below its critical temperature enhanced the pinning of magnetic domains drastically [Fig. 5(b)]. It should be emphasized that further investigations proved this effect to be independent of the particular position above the superconductor. Since niobium is a type-II superconductor and demagnetization effects are large for thin S films in perpendicular external fields,[18,19] vortices certainly penetrate the superconductor at the base temperature. In the present case, the density of penetrating vortices was rather high, as fields of several hundreds of millitesla were measured above the S film. Moreover, superconducting niobium films often exhibit strong intrinsic pinning for magnetic-flux tubes,[20] due to inhomogeneities in the material where superconductivity is less favorable.

With these considerations in mind, the enhancement of the pinning of magnetic domains by the superconductor can be understood as follows. When cooling the S/F hybrid to the base temperature at a certain external magnetic field, vortices appear in the superconductor according to the actual configuration of the underlying magnetic domains. Now, while keeping the temperature fixed, the magnetic domains tend to rearrange upon changes in the external field. For such rearrangement, magnetic domain walls have to be moved, together with the vortices close to the domain walls. Since the vortices are attached to intrinsic pinning centers in the niobium film, their movability is hampered, which is an obstacle to the movement of the magnetic domains. However, when the temperature increases above T_c, the additional pinning of the magnetic domains that is caused by the superconductor disappears, allowing the domains to reach their new favorable distribution. Therefore, *the presence of the superconductor reduces the mobility of the magnetic domains in the ferromagnetic substrate.*

It might also be possible that vortices cannot leave the superconductor when decreasing the external field at the base temperature, resulting in a vortex critical state in the beginning of the first imaging sequences of the above described experiment. In that case, in the vicinity of the superconductor, the ferromagnetic substrate would not experience the change in the external field until T increases sufficiently so that the flux can leave the niobium film. In Fig. 4 we present the differences $\Delta_{1,2}$ and $\Delta_{2,1}$ between the averages of $B_{\mathrm{Hall}}(5\ \mathrm{K})$, obtained during the first and second imaging sequences at the same external field and during the second and first sequences at subsequent external fields, respectively. Clearly, $\Delta_{2,1} \sim 5$ mT for most values of H_{ext}, indicating that already most of the flux left the superconductor at 5 K upon reducing H_{ext} at the base temperature. Accordingly, values of $\Delta_{1,2}$ concentrate around 0 mT. These findings support the interpretation that the observed reduced mobility of the magnetic domains is due to the above described vortex-mediated pinning rather than to flux repulsion by the superconductor in the critical state.

In conclusion, the present study provides direct experimental evidence for the influence of the superconductor on the ferromagnet in a S/F hybrid system. It was found that below its critical temperature, the superconductor reduces the mobility of the magnetic domains. This effect was explained by the immobilization of magnetic domains via vortices, which are pinned to intrinsic inhomogeneities in the super-

conductor. Such explanation is entirely analogous to the famous example of a levitating superconductor that moves along a magnetic path: in that case, the superconductor cannot leave the track even in a turn, since for this to do, vortices must be detached from the intrinsic pinning centers of the superconductor. In the present experiment, just the inverse of the above example happens, as the superconductor is fixed while magnetic domains try to move.

This work is supported by the FWO, GOA, and IAP projects and the ESF-NES Research Networking Programme.

*joachim.fritzsche@fys.kuleuven.be

[1] A. I. Buzdin, Rev. Mod. Phys. **77**, 935 (2005).
[2] I. F. Lyuksyutov and V. L. Pokrovsky, Adv. Phys. **54**, 67 (2005).
[3] F. S. Bergeret, A. F. Volkov, and K. B. Efetov, Rev. Mod. Phys. **77**, 1321 (2005).
[4] Z. Yang, M. Lange, A. Volodin, R. Szymczak, and V. V. Moshchalkov, Nature Mater. **3**, 793 (2004).
[5] L. N. Bulaevskii, E. M. Chudnovsky, and M. P. Maley, Appl. Phys. Lett. **76**, 2594 (2000).
[6] M. V. Milosevic and F. M. Peeters, Phys. Rev. B **68**, 094510 (2003).
[7] L. E. Helseth, P. E. Goa, H. Hauglin, M. Baziljevich, and T. H. Johansen, Phys. Rev. B **65**, 132514 (2002).
[8] L. N. Bulaevskii and E. M. Chudnovsky, Phys. Rev. B **63**, 012502 (2000).
[9] E. B. Sonin, Phys. Rev. B **66**, 136501 (2002).
[10] I. F. Lyuksyutov and V. L. Pokrovsky, Adv. Phys. **57**, 67 (2005).
[11] S. V. Dubonos, A. K. Geim, K. S. Novoselov, and I. V. Grigorieva, Phys. Rev. B **65** 220513(R) (2002).
[12] C. Monton, F. de la Cruz, and J. Guimpel, Phys. Rev. B **75**, 064508 (2007).
[13] S. J. Bending, Adv. Phys. **48**, 449 (1999).
[14] R. J. Gambino and F. Leonhard, J. Am. Ceram. Soc. **44**, 221 (1961).
[15] R. Szymczak, Acta Phys. Pol. A **43**, 571 (1973).
[16] A. Hubert and R. Schäfer, *Magnetic Domains—The Analysis of Magnetic Microstructures* (Springer-Verlag, Berlin, Heidelberg, 1998), Chap. 3, p. 330.
[17] T. Jourdan, F. Lancon, and A. Marty, Phys. Rev. B **75**, 094422 (2007).
[18] F. M. Araujo-Moreira, C. Navau, and A. Sanchez, Phys. Rev. B **61**, 634 (2000).
[19] W. T. Norris, J. Phys. D **3**, 489 (1970).
[20] G. S. Park, C. E. Cunningham, B. Cabrera, and M. E. Huber, Phys. Rev. Lett. **68**, 1920 (1992).